Water Science & Technology

Water Science & Technology Vol 84 No 5, 1257 doi: 10.2166/wst.2021.314

Adsorption and migration of heavy metals between sediments and overlying water in the Xinhe River in central China

Yanqi Zhao [a,*], Ying Yang[a], Rongkun Dai[a], Sobkowiak Leszek[b], Xinyi Wang[a] and Lizhi Xiao[a]

[a] Institute of Resources & Environment, Henan Polytechnic University, Jiaozuo 454003, China
[b] Institute of Physical Geography and Environmental Planning, Faculty of Geographical and Geological Sciences, Adam Mickiewicz University, Poznań 61-680, Poland
*Corresponding author. E-mail: zhaoyq@hpu.edu.cn

YZ, 0000-0001-5630-8248

ABSTRACT

Long-term polluted rivers often lead to the accumulation of heavy metals in sediments. Anthropogenic activities or biological disturbances break the adsorption balance, causing them to return from the bottom mud to the overlying water and change the aquatic environment. In order to understand the variation of heavy metals between sediments and river water, we collected the riverbed sediments in the polluted Xinhe River and carried out static continuous infiltration and dynamic uninterrupted disturbance experiments. The leaching experiment shows that the absorbability of Cd and Pb is stronger than Cr in the sediment; at the same time, the properties of the medium have a great influence on the adsorption of heavy metals. The disturbance can prompt heavy metals in the sediment to resuspend into the overlying water. The impact is the greatest during the first 12 h, and the influence degree is stronger in the relatively static water than in the moving river. In addition, pH and other factors have different degrees of influence on the desorption of heavy metals.

Key words: disturbed experiment, heavy metal, infiltration, migration, overlying water, sediment

HIGHLIGHTS

- The static infiltration and dynamic agitation experiments were carried out.
- The adsorption performances of Cd and Pb were better than that of Cr.
- Disturbances greatly affect heavy metals in sediments especially at the first 12 h.
- Disturbance has irregular effect on Fe and Cu in sediments.
- Influence of disturbance in static water on heavy metals is greater than that in flowing water.

GRAPHICAL ABSTRACT

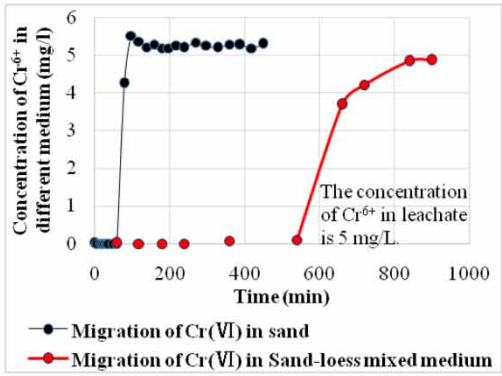

Vertical migration of Cr^{6+} in different media.

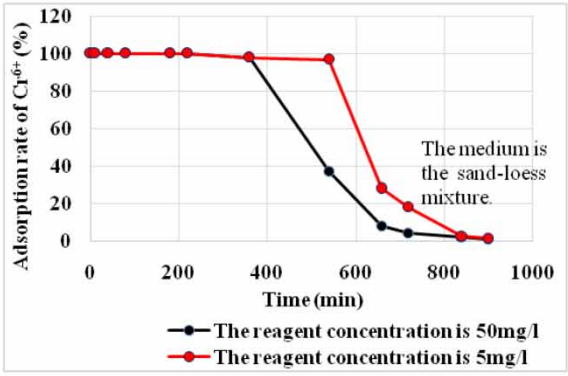

Change of adsorption rate for Cr^{6+} with different concentration in sand-loess media.

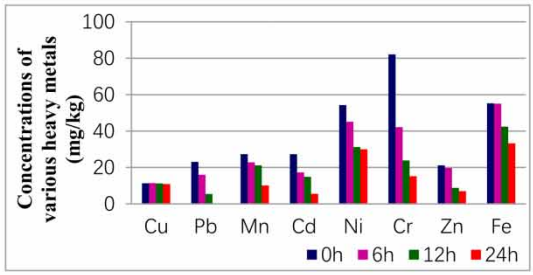

The content Change of Cu, Cd, Fe, Pb, Ni, Cr, Zn and Mn in the downstream sediment with simulating water flow during the disturbance experiment.

1. INTRODUCTION

The increase in population and the rapid development of industrialization and urbanization have led to heavy metal contamination in the environment, such as pollutants emitted into the atmosphere from the combustion of energy materials, sewage discharged from mining, smelting, various chemical industries, irrigation, domestic, and leachate from landfills (Hu *et al.* 2014). Because of their persistence, high toxicity, bioaccumulation, non-degradability, and their ubiquitous nature (Zhang *et al.* 2018; Hassimi *et al.* 2019), heavy metal pollution is an exceedingly hazardous environmental problem (He *et al.* 2019), particularly in disturbing the normal functions of the water environment, soil, and biosphere. In the special project 'The 12th 5-Year Plan for Comprehensive Prevention and Control of Heavy Metal Pollution' (2011–2015) issued by the Chinese government, five major heavy metals (Cr, Cd, Pb, Hg, and As) have been selected as priority pollution elements to be controlled (Hu *et al.* 2014). These heavy metals can accumulate through the biological chain and enter the human body

through food, causing dysfunction, such as in the nervous and cardiovascular systems, and even cancer. According to the environmental quality standards for surface water (GB 3838-2002, currently being implemented), the allowable limits of the heavy metals in class IV water are: Cr^{6+} ≤0.05 mg/L, Cd ≤0.005 mg/L, Pb ≤0.05 mg/L, Hg ≤0.001 mg/L, and As ≤0.1 mg/L. The sanitary standards for drinking water (GB 5749-2006, currently being implemented) stipulated the following limits: Cr^{6+} ≤0.05 mg/L, Cd ≤0.005 mg/L, Pb ≤0.01 mg/L, Hg ≤0.001 mg/L, and As ≤0.01 mg/L.

At present, a large amount of heavy metals has entered into rivers, lakes, and other water bodies (Shi & Zhang 2018; Zhang *et al.* 2018). All types of water bodies are an important connection between the geosphere and biosphere, especially playing a major role in transporting heavy metal pollutants. Globally, heavy metal loads in the aquatic ecosystems are on the rise (Martin *et al.* 2015; Amankwaa *et al.* 2021). The heavy metals discharged in the water bodies through different sources would eventually be enriched in the sediments by adsorption, complexation, flocculation, and sedimentation (Zhang *et al.* 2018). So, the sediments serve not only as a primary settling accumulation field and a carrier of heavy metals, but they also reflect their contamination level (Tang *et al.* 2014; Guan *et al.* 2018; Lu *et al.* 2019).

Compared with the hydrostatic condition, the heavy metals in the sediment are more likely to migrate under dynamic water conditions (Shi & Zhang 2018). Once the water environmental conditions change, the dynamic equilibrium between the sediment and the water interface will be broken, so that the heavy metals in the sediment will be transferred and transformed and released to the overlaying water (Zhang *et al.* 2018). Thus, sediment resuspension, redox reaction, and desorption can usually become potential sources of recontamination (Jafarabadi *et al.* 2018). The power source resulting in changes of the sedimentary conditions is divided into natural factors and anthropogenic perturbations. The natural factors mainly include hydrodynamics (e.g., wind wave, storm, tide (Lin *et al.* 2019; Lu *et al.* 2019), and water flow), chemical processes, and bioturbation (Song *et al.* 2015). The man-made factors mainly include ship transportation (Superville *et al.* 2014), sand mining, dredging operations, fishing, and other human activities (Shi & Zhang 2018). Meanwhile, sediments are also complex and diverse, with different physical and chemical properties. A large number of studies have found that the release of heavy metals in the sediment is synthetically affected by environmental conditions, such as temperature, pH, salinity, dissolved oxygen, redox potential, and other factors (Jafarabadi *et al.* 2018; Shi & Zhang 2018).

Therefore, some scholars have carried out investigations on heavy metal pollution in a certain watershed and evaluated the degree of pollution with certain evaluation methods (Tang *et al.* 2014; Song *et al.* 2015; Guan *et al.* 2018). However, more researchers are focusing on the removal methods of heavy metals by adsorption materials and their influencing factors (Abdelhay *et al.* 2018; Al-Ananzeh 2021; Chen & Pan 2021). Simultaneously, some people also have set up leaching adsorption experiments (Won *et al.* 2019; López *et al.* 2020) or resuspension experiments (Shi & Zhang 2018; Hassimi *et al.* 2019; Lu *et al.* 2019) of heavy metals.

It is complicated and difficult to analyze the migration of heavy metals between the overlying water and the benthic sediment and also in the subsurface flow zone below the riverbed from river water to groundwater (Basack *et al.* 2014). Based on the importance and specificity of aquatic ecosystems, in order to accurately grasp the adsorption and desorption characteristics of heavy metals between the sediment and the overlying water under changing hydrodynamic conditions and their influencing factors, in this study, static leaching experiments were used to explore the adsorption properties of heavy metals from the polluted water to the bottom sediments, and dynamic disturbance experiment was used to study the re-suspension migration of heavy metals from the bottom mud and their influencing factors.

2. METHODS

2.1. Overview of study area

Jiaozuo (113°4′–113°26′E, 35°10′–35°21′N) is a prefecture-level city located in the northwestern part of Henan province, North China (Figure 1). It has a population of 3.56 million and used to be an industrial and mining city with abundant coal resources. The study area, along the Xinhe River, is located in the south of Taihang Piedmont and the northwest of the Yellow River alluvial plain. It is composed of Piedmont alluvial fan and Piedmont depression, which is covered by Quaternary sediments. The lithological compositions are mainly silt, silty clay, and fine sand. The Xinhe River, the main discharge channel for industrial and mining enterprises and urban sewage of Jiaozuo City in the past, has a total length of 19.5 km and a catchment area of 272 km^2. It collects waters of several seasonal rivers flowing through the urban area, such as the Puji, Qunying, and Wengjian Rivers (Figure 2), and finally merges into the Haihe River water system. We collected the water samples at five representative sites located along the Xinhe River (Figure 2), namely at the headwaters, estuary, and

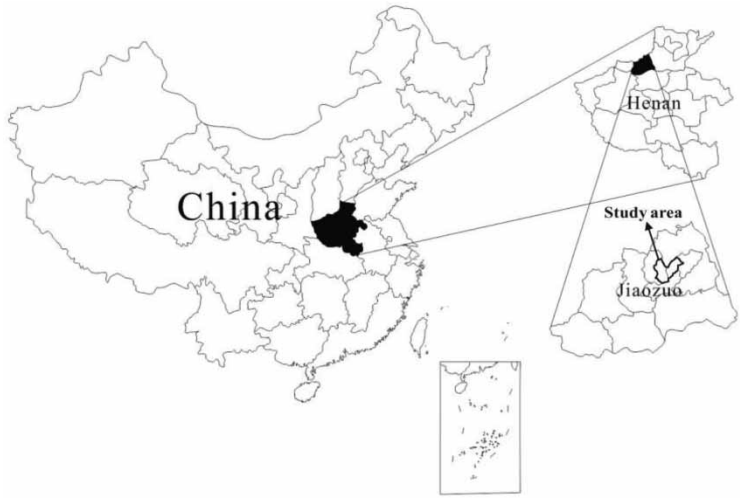

Figure 1 | Location of the study area.

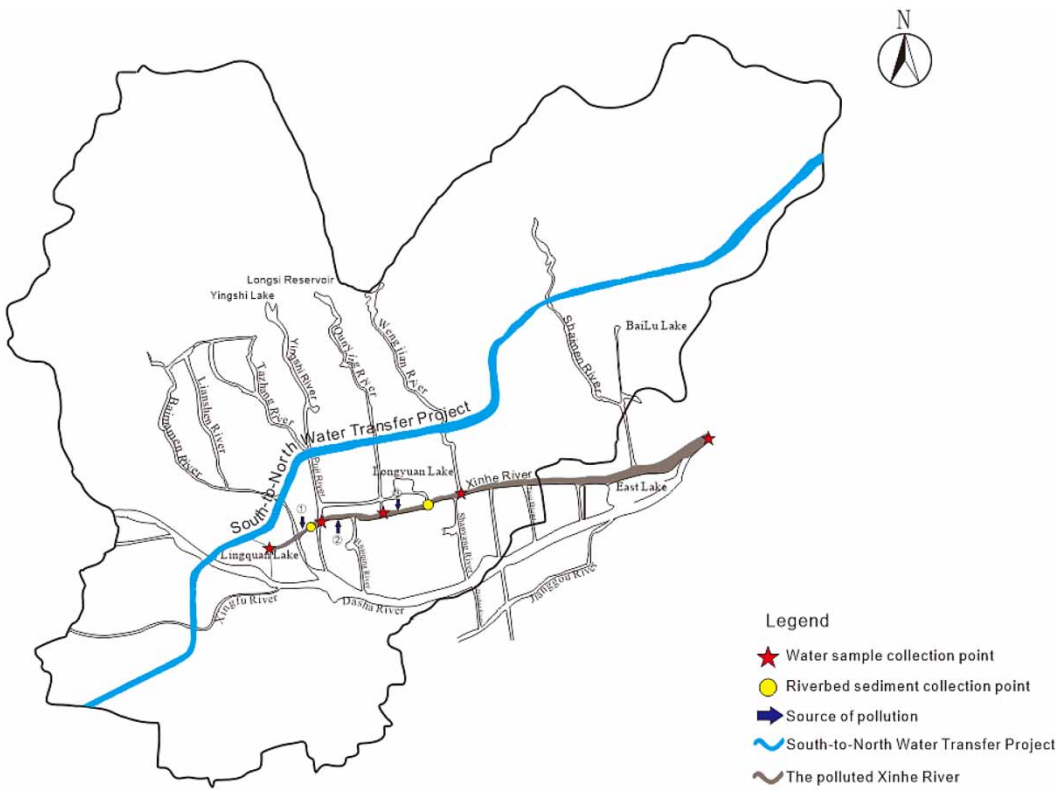

Figure 2 | River system of Jiaozuo City and localization of the sample collection points.

confluences with its three tributaries, respectively. Through the routine laboratory analysis of the water samples (Table 1), it is known that the main pollutants of the Xinhe River are nutrients and chemical oxygen demand (COD). Heavy metals cause mild pollution, but their concentration in the estuary is close to the national standard limit. Additionally, the Xinhe River pollution is mainly influenced by three seasonal rivers flowing through the urban area. The field investigation reveals that the garment, electronics and hardware processing factories, mines, hospitals and farms located in the vicinity of the three rivers and along the Xinhe River mainstream are main sources of pollution.

Table 1 | Results of routine analysis of water samples in the Xinhe River (mg/L)

Sampling point	pH	COD	NH_3-N	TP	F^-	Cl^-	Pb	Cd	Cr^{6+}
Headwaters of Xinhe River	6.5	25	4	0.2		226.7	0.06	0.002	0.003
Estuary of Puji River	7.4	196	11	0.4	0.816	128	0.085	0.006	0.02
Estuary of Qunying River	7.3	152	11.4	3.5	0.485	480	0.051	0.003	0.01
Estuary of Wengjianhe River	7.7	145	10.1	2.4	0.756	345	0.076	0.008	0.02
Estuary of Xinhe River	7.1	205	22	3.1		14.1	0.11	0.009	0.095
Standard (Class V)[a]	6–9	40	2.0	0.4	1.5	250	0.1	0.01	0.1

[a]The State Standard of the People's Republic of China: Environmental quality standards for surface water (GB 3838-2002). Class V: water is suitable mainly for agricultural areas and areas with general landscape requirements.

Since the South-to-North Water Transfer Project ensuring safe water use in North China runs close to the Xinhe River, and also due to the governmental policy striving for creation of a national civilized and ecological city, Jiaozuo City has recently invested a considerable amount of funds in the reconstruction of the city's water system to improve long-term polluted rivers. However, the hydro-technical works aiming to repair the watercourses will inevitably result in the resuspension of riverbed sediment and the subsequent migration and transformation of heavy metals.

2.2. Sediment sample preparation

The sediment samples were collected in July 2018 from the upper and middle parts of the Xinhe River (Jiaozuo City, China) (Figure 2). Sediments were taken with a columnar sampler from 0 to 10 cm deep from each point below the riverbed. The collected core sediments were placed in labeled polyethylene decontaminated containers (Amankwaa *et al.* 2021) and transported to the laboratory for natural air-drying. Then, a 1 mm sieve was used to sift dry sediment. At the same time, the sifted samples were analyzed by the Rise-2006 laser particle size analyzer for determining particle size and other parameters (Table 2).

2.3. Experimental apparatus and process

2.3.1. Static infiltration experiment

The lixiviation set-up consists of two devices, a one-dimensional permeation cylinder and a two-dimensional penetration cube (Figure 3). The cylindrical device is 10 cm in diameter and 55 cm in the sand filling height. Water samples in the experimental process are uniformly extracted from the lower sampling hole 35 cm below the sand surface. The cuboids device is 120 cm long, 20 cm wide, and 60 cm high. It is used to simulate the process of the two-dimensional vertical infiltration and lateral migration of river pollutants in the riverbed media. The four sampling holes on the panel are equally distributed, and the right and left sampling holes are correspondingly used to monitor the upstream and downstream seepage of the simulated river. Since the concentration of heavy metals in the two lower sampling holes could not be detected during the whole

Table 2 | Physical and hydro-geological parameters of the media used in the experiment

	Share of particle size (%)				
Media type	**0.25–0.5 mm**	**0.075–0.25 mm**	**0–0.075 mm**	**Median of particle size (mm)**	**Specific surface area (m^2/g)**
Fine sand	57.42%	41.12%	1.46%	0.453	0.004
Coarse sand	55.28%	42.78%	1.94%	0.536	0.0033
Loess	71.45%	24.78%	3.77%	0.34	0.0053
Media type	**Porosity**	**Bulk specific gravity (g/cm^3)**	**Specific gravity (g/cm^3)**	**Saturated moisture content (%)**	**Permeability coefficient (cm/s)**
Fine sand	0.376	1.59	2.55	11.40	0.0077
Coarse sand	0.43	1.45	2.58	11.30	0.0079
Loess	0.35	1.61	2.48	24.95	0.00043

Figure 3 | Infiltration experimental apparatus (left: cylindrical, one-dimensional, vertical infiltration column; right: box-shaped, two-dimensional infiltration tank).

experiment, water samples for further analyses are extracted only from the two upper sampling holes (15 cm below the surface of the simulated riverbed).

According to the survey results of heavy metal contamination in the study area, Cr^{6+}, Cd, and Pb were selected as the reagents for the percolation experiments. Based on the different adsorption properties of the three heavy metals, we prepared a solution containing 5 mg/L Cr^{6+}, and a mixed solution containing Cr^{6+}, Cd, and Pb (the concentration of each metal element is 50 mg/L). Leaching experiments were respectively carried out with these two sets of solutions. The filling medium in the experimental devices was divided into three groups: the one-dimensional cylindrical column filled separately with homogeneous fines and samples and a mixture of fine sand, coarse sand, and loess (in mass ratio 1.5: 1.5: 1), and the cubic device filled with homogeneous fine sand samples. The leaching media used in the experiment was the fresh riverbed sand and the river bank loess (Table 2). After being dried and sieved, they were put into the two devices and compacted. The saturated leaching was carried out once with pure water, and then the simulated infiltration experiments started to operate with the prepared leachate.

The leaching experiment was first conducted with a solution containing Cr^{6+} (5 mg/L) in the three media. After that, they were carried out with the mixed solution of Cr^{6+}, Cd, and Pb of 50 mg/L. During the whole leaching experiment, the upper surface of the cylindrical column maintained a liquid level that was 5 cm high, while in the box-shaped tank, it was 1 cm, and the liquid flows from right to left.

2.3.2. Dynamic disturbance experiment

In order to simulate the release of heavy metals from the riverbed sediment under disturbance, we designed a set of dynamic disturbance apparatus (a flume turbulence device) (Figure 4). The water tank is 30 cm long, 25 cm wide and 10 cm high. The glass pipes are respectively connected to its front and rear ends at a height of 7 cm. The front rubber hose is connected with the faucet and a flow meter (LZB-3, Double wave instrument factory in Changzhou, Jiangsu), and a mechanical stirrer (STSJB-1000, SUOTN Experimental Instruments Co., Ltd in Shanghai) is placed above the water tank. At the bottom of the tank, a 4.5 cm thick layer of the previously collected sludge samples was evenly laid, and then water was slowly added to maintain a height of 2.5 cm.

For the experiment, two kinds of in-situ sediments were used, and two different scenarios were set up to carry out four combinations of river/reservoir disturbance simulation experiments (i.e., the agitation of the upstream and downstream samples in static water (simulating a reservoir or pond) and a flowing state (simulating a river)). The mud sample was spread on the bottom of the tank, and the experiment was individually carried out in four scenarios so as to observe changes of the heavy metal content in the sediments after different water bodies were disturbed. The influence of the parameters of the water

Figure 4 | Dynamic disturbance experimental apparatus.

solution was determined. The speed of the mechanical agitator was set at 200 r/s, and the water flow rate was controlled and set at 0.07 m/s by the flow meter.

Based on the observations and measurements, it is concluded that the lower reaches of the Xinhe River are more polluted than its upper reaches. For the two test samples, the initial pollution levels of Cu, Cd, Cr, and Ni are higher in the downstream sediment samples, while these of Pb, Zn, and Mn are higher in the upstream samples. The Fe content is basically the same in the upstream and downstream samples. The water and mud samples of 15 mL were taken to analyze the concentration of each heavy metal at the beginning of the experiment and after 6, 12, and 24 h. Before each sampling, the agitator and water flow were turned off, and the sample was allowed to stand for 10 min. Then, the sedimentary mud samples in the corresponding experimental sampling period were collected.

2.4. Quality control and quality assurance

The REDOX potential, pH, water conductivity, and dissolved oxygen were measured by the portable multi parameter analyzer (DZB-718 L) produced by the Leici Experimental Instrument Co., Ltd (Qingdao of Shandong, China). After the probe was placed in the solution for 5 min, a steady reading was taken. The organic matter of the mud sample was measured by the total organic carbon analyzer (TOC-5000) produced by Shanghai Metash Instruments Co., Ltd (China). The heavy metals Fe, Cu, Pb, and Cd were measured by a flame atomic absorption spectrometer (AAS8510) produced by Meicheng Precision Instrument Co., Ltd (Shenzhen of Guangdong, China), while Mn, Ni, Cr, and Zn were determined by an inductively coupled plasma optical emission spectrometer (ICP-OES) produced by NCS Testing Technology Co., Ltd (Beijing, China). The sludge digestion process was set to a power of 600–800 W and allowed to react for 10 min at 130 °C, 5 min at 150 °C, and 10 min at 180 °C. After the reaction, the instrument was automatically cooled down to 60 °C, and then the sample was taken out for acid removal.

3. RESULTS AND DISCUSSION

3.1. Migration characteristics of heavy metals in leaching experiment

In the cylindrical vertical infiltration model, the percolation rate of Cr^{6+} in the homogeneous sand was much higher than that in the sand–loess mixture. Figure 5-left shows that the migration speed drops rapidly after 25 min in the pure sand, and the concentration in the medium reached 75% (3.7 mg/L) of the leachate concentration. After that, the concentration in the sediment increased slowly and finally was stabilized. In the box infiltration model, it took about 80 min to reach saturation (Figure 6). Nevertheless, in the sand–loess medium, the migration speed decreased after 550 min, and the concentration in the mixed medium reached 73.68% (3.684 mg/L) of the leaching reagent after 660 min. Compared with the homogeneous sand, the rate curve in the mixed medium increased gradually to the saturation level rather than within a short time. By analyzing the two media with the particle imaging system, it was determined that the porosity of the sand–soil mixed media with two different particle sizes is lower than that of the pure sand media, but the specific surface area is larger. This indicates that the vertical migration of Cr^{6+} is mainly affected by the permeability coefficient and the amount of water passing through the media (Wang *et al.* 2020). In addition, Figure 5-right indicates that the adsorption saturation time of Cr^{6+} was about 200 min

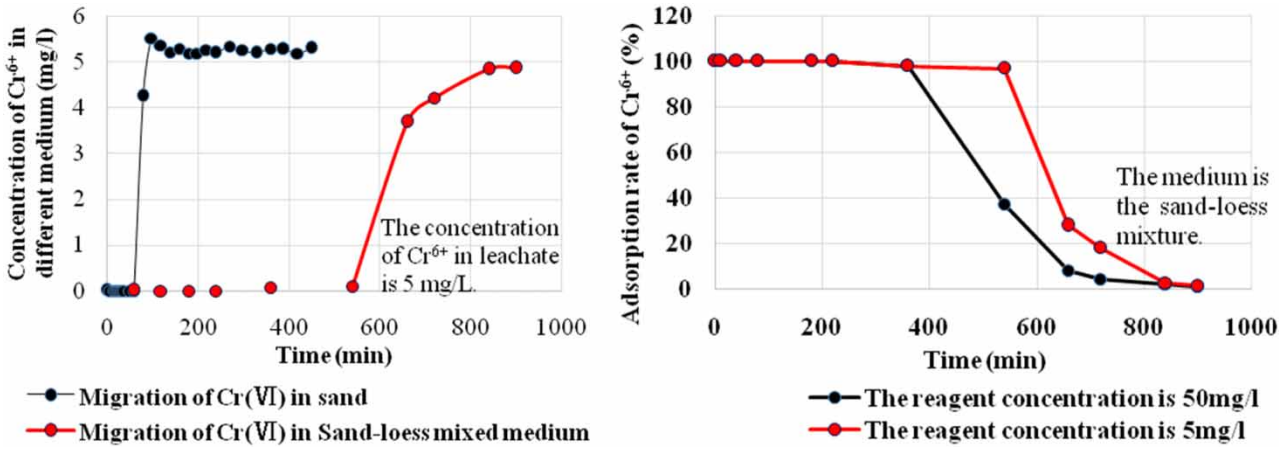

Figure 5 | Vertical migration of Cr^{6+} in different media (left) and adsorption rate for Cr^{6+} with different concentrations in sand–loess media (right) in the cylindrical leaching experiment.

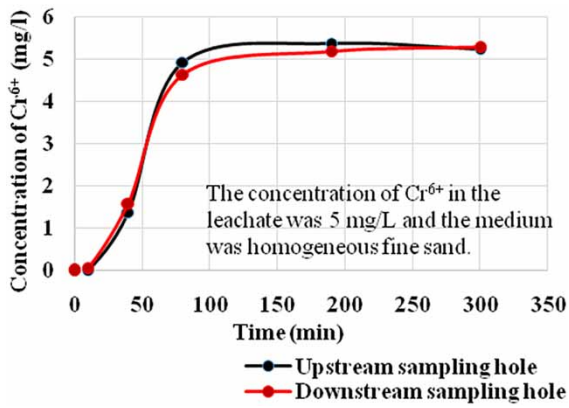

Figure 6 | Two-dimensional migration of Cr^{6+} in homogeneous sand media.

shorter when the reagent concentration was increased ten times in the infiltration experiment with the mixed sand–loess medium. This means that the adsorption capacity is also driven by the concentration gradient of the adsorbates (Chen & Pan 2021).

Regarding Cd and Pb, the downward migration is so difficult that it was almost impossible to detect their concentrations in the sampling sites at the depth of 15 cm even in homogeneous sand after one day of the leaching experiment. This is mainly because they are the most strongly sorbed metals and are governed by the composition of the surface solid phase, besides the effects of solution chemistry (e.g., pH, metal speciation, ionic strength). Simultaneously, by comparing the horizontal and vertical migration in the experiment with the simulating river equipment, it was determined that horizontal migration and lateral infiltration along the river are far greater than vertical infiltration (Zhao & Yang 2007). This also confirms the above conclusion. So, once the river is polluted long-term, it will have a greater impact on the depositional environment and soil both on banks and downstream.

3.2. Characteristics of heavy metals in riverbed sediments under different circumstances of the perturbation experiment

The experimental results show that Pb of the downstream sample in the static water conditions and Cd of the upstream sample in the flowing water were not detected in the sediment after stirring for less than 6 h (Figure 7(b) and 7(c)). Cr,

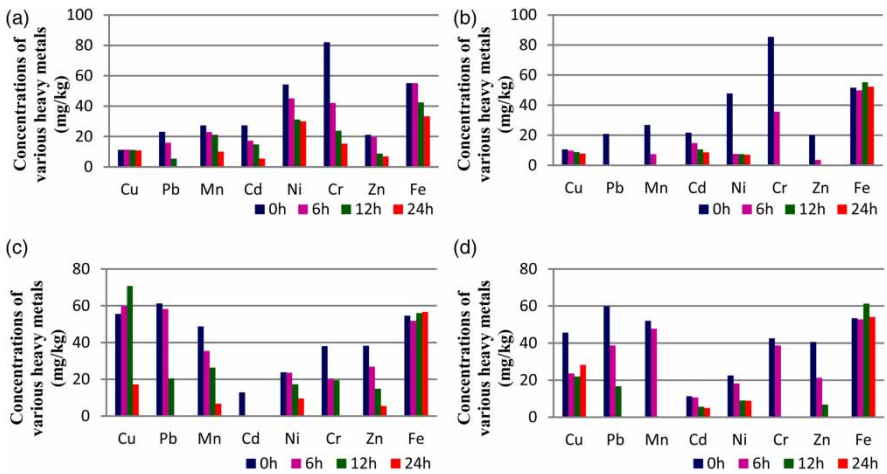

Figure 7 | The concentration change of Cu, Cd, Fe, Pb, Ni, Cr, Zn, and Mn in the sediment during the disturbance experiment. (a) Downstream sediment samples in the flow state; (b) downstream sediment samples in still water; (c) upstream sediment samples in the flow state; (d) upstream sediment samples in still water.

Table 3 | Correlation analysis between heavy metals and physical–chemical properties of sediments during disturbance experiments

Metals	Disturbance experimental scenario	pH	Eh	DO	Conductivity	TOC
Cu	Downstream sediments in moving water	−0.684	0.912	−0.093	0.300	−0.932
	Downstream sediments in standing water	0.868	−0.172	0.771	−0.944	−0.771
	Upstream sediments in moving water	0.067	0.550	−0.422	0.055	0.991**
	Upstream sediments in standing water	−0.286	0.941	−0.946	−0.617	−0.348
Fe	Downstream sediments in moving water	−0.803	0.96*	0.218	0.460	−0.733
	Downstream sediments in standing water	−0.280	0.508	−0.204	0.175	0.012
	Upstream sediments in moving water	0.041	−0.396	0.528	0.008	−0.482
	Upstream sediments in standing water	−0.694	−0.964*	0.229	0.435	0.942
Zn	Downstream sediments in moving water	−0.814	0.996**	0.449	0.523	−0.582
	Downstream sediments in standing water	0.993**	0.383	0.993**	−0.735	−0.388
	Upstream sediments in moving water	0.723	−0.923	−0.988*	0.737	0.479
	Upstream sediments in standing water	0.011	0.433	−0.571	−0.975*	−0.560
Ni	Downstream sediments in moving water	−0.905	0.553	0.452	0.708	−0.499
	Downstream sediments in standing water	0.975*	0.524	0.999**	−0.682	−0.330
	Upstream sediments in moving water	0.432	0.153	−0.862	0.447	0.719
	Upstream sediments in standing water	0.251	0.562	−0.441	−0.974*	−0.740
Cr	Downstream sediments in moving water	−0.977*	0.917	0.302	0.867	−0.499
	Downstream sediments in standing water	0.971*	0.140	0.932	−0.798	−0.485
	Upstream sediments in moving water	0.740	−0.172	−0.926	0.740	0.616
	Upstream sediments in standing water	0.416	0.560	−0.270	−0.995*	0.818
Cd	Downstream sediments in moving water	0.982*	0.812	0.029	0.804	−0.744
	Downstream sediments in standing water	0.868	−0.172	0.771	−0.944	−0.771
	Upstream sediments in moving water	0.995**	−0.734	−0.869	0.996**	0.022
	Upstream sediments in standing water	0.363	0.487	−0.264	−0.975*	−0.766
Mn	Downstream sediments in moving water	−0.891	0.934	−0.129	0.626	−0.899
	Downstream sediments in standing water	0.992**	0.283	0.975*	−0.770	−0.436
	Upstream sediments in moving water	0.667	−0.094	−0.949	0.674	0.628
	Upstream sediments in standing water	0.420	0.557	−0.262	−0.954*	−0.818
Pb	Downstream sediments in moving water	−0.926	0.989*	0.307	0.688	−0.644
	Downstream sediments in standing water	0.973*	0.533	0.998**	−0.673	−0.318
	Upstream sediments in moving water	0.502	0.015	−0.910	0.523	0.564
	Upstream sediments in standing water	0.055	0.339	−0.450	−0.995**	−0.550

*Correlation significant at 0.05 level (both sides).

**Correlation significant at 0.01 level (both sides).

Mn, and Zn (except for the upstream sample of Zn after at least 12 h (Figure 7(d))) were also absent in the two types of sediments in the static water stirred for 6 h (Figure 7(b) and 7(d)). The comparison of the disturbance experiment results in the two states reflects that the heavy metals in the sediment of the flowing water were more stable than that of the static water after disturbance, except for a special case of Cd. Regardless of the sediment or experimental conditions, the desorption rate of Pb and Cr (except for Figure 7a) was faster, and they were not detected in the sediment after 12 h. At the same time, from the perspective of the degree of desorption, the desorption rate of Pb, Zn, Mn, and Cr in the sediments continued to increase rapidly with the increase in disturbance time. In the four experimental scenarios, according to the degree of concentration decrease over time, the desorption rate of heavy metals were respectively shown in the following order: Pb > Zn > Mn > Cr > Ni > Cd > Cu (Fe is irregular) for the two experimental scenarios of the downstream sediment sample; Cd > Pb > Cr > Zn > Mn > Ni (Fe and Cu is irregular) for the upstream deposition sample in the presence of water flow experimental scenario; Mn > Cr > Pb > Zn > Ni > Cd (Fe and Cu is irregular) for the upstream deposition sample in static water. This may be related to the activity of different metals in different sediment and water flow states. On the whole, the heavy metal de-sorption rate was the fastest in the first 12 h in all scenarios, and then gradually stabilized until it partially disappeared.

Factors such as pH, redox potential (Eh), dissolved oxygen (DO), conductivity, and organic matter contents (TOC) in the sedimentary environment greatly influence the distribution and migration of heavy metals in sediments. With the help of the Pearson correlation analysis between the heavy metal content in the sediment and the physical–chemical factors under different experimental conditions, we found that pH has a positive effect on the content of most heavy metals in the sediments of still water (Table 3). In general, the heavy metals can achieve high desorption from the sediment at low pH values (Pedersen *et al.* 2017; Adenuga *et al.* 2019; Kobayashi *et al.* 2020). In our experiment, the sedimentary environment is more acidic than the overlying water environment (the pH column in Figure 8 was below the polygonal line). Meanwhile,

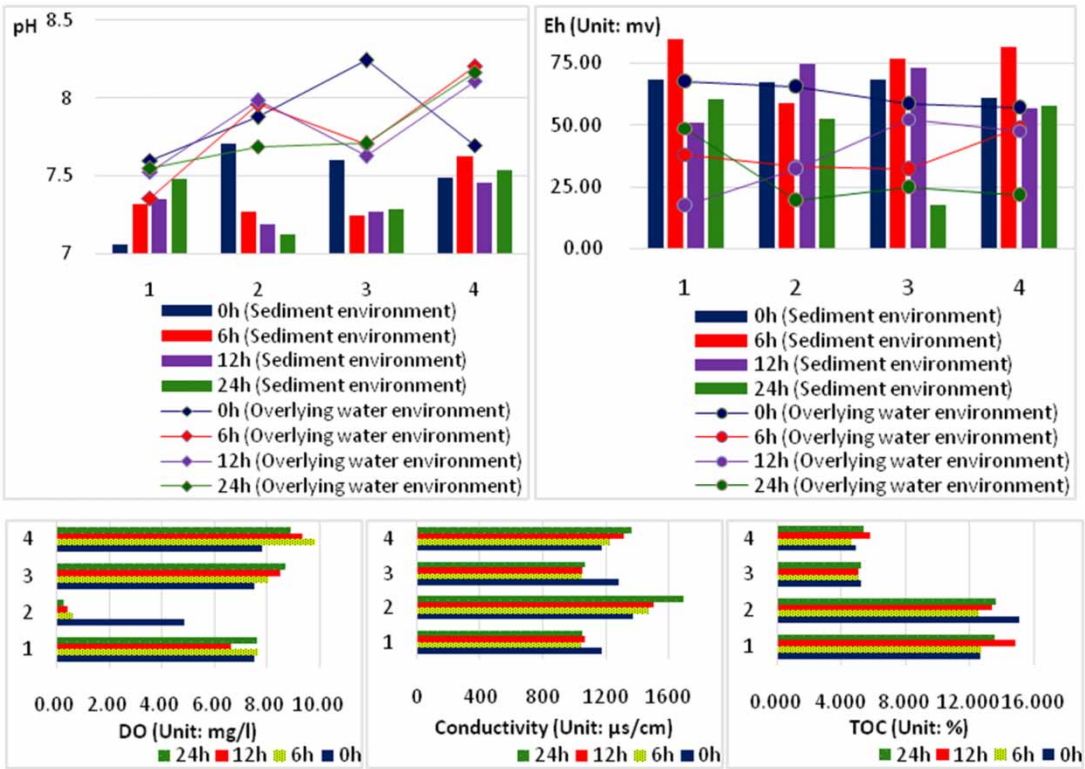

Figure 8 | Changes of physical–chemical properties of sediment samples in different scenarios. *Note*: '1'and '2' on the axis refer to the sediment samples collected from the downstream individually under the simulated water flow and the static water conditions; '3' and '4' refer to those collected from the upstream, respectively, under the simulated water flow and the static water conditions.

Eh has a positive effect on their content in the sediments of disturbed water. (It can be seen from the correlation coefficient being greater than 0.9 in Table 3 and the column higher than the dotted line in Figure 8.) The predominant mechanisms of Eh are ionic exchange. DO is positively correlated with the heavy metal content of downstream sediment samples in still water but negatively correlated with the content of upstream samples under water flow disturbance (Table 3). Except for the large reduction in DO in Scenario 2, the rest was basically stable at 7–10 mg/L (Figure 8). There is a linear negative correlation between the conductivity and concentration (Chu *et al.* 2018) of most heavy metals in the downstream sediments of still water (Table 3). In the case of the simulated water flow, the conductivity in the water environment suddenly decreased after disturbance for 6 h, and then there was basically no change in the subsequent experimental time (Scenarios 1 and 3 of the conductivity histogram in Figure 8), but Scenarios 2 and 4 (under no water flow) showed a gradual increase in conductivity with increasing experiment time. Regarding TOC, the value of the downstream sample (1 and 2 in Figure 8) was 3–4 times that of the upstream sample (3 and 4 in Figure 8), and during the whole experimental process, it did not change much.

3.3. Important rules obtained from the experiment and their practical application value

Through a series of experiments, we found that most heavy metals had strong adsorption and weak vertical migration ability in the sediment, especially for the medium with complex components. However, once they are disturbed by biology or human activities, many heavy metals, such as Pb, Cr, and Mn in the sediments would soon be desorbed from the sediment and re-released into the river. In particular, the impact was the greatest during the first 12 h and then decreased quickly. The degree of desorption was closely related to the categories and properties of the heavy metals and the physical–chemical characteristics of their surrounding environment. Once the heavy metals accumulated in the sediment, they would become the main source of re-pollution of the river. So, river managers should focus their attention on preventing rivers from being polluted by heavy metal-containing sewage and to specially treat the black and foul-smelling rivers during the sediment cleaning process.

4. CONCLUSIONS

In this research, we collected sediments from the Xinhe River (a perennial polluted river in Jiaozuo City, China) and carried out static vertical and two-dimensional infiltration experiments of heavy metals and dynamic disturbance experiments. The infiltration experiment proved that the adsorption performances of Cd and Pb were better than that of Cr, especially for compact and small size sediments. Through the disturbance experiment, it was determined that the disturbance can promote the release of heavy metals from the sediments into the overlying water in a short time. The effect of disturbance on the desorption of heavy metals in the sediment is relatively greater in stationary water than in flowing water.

ACKNOWLEDGEMENTS

The authors would like to thank editors and reviewers for their helpful suggestions. This research was jointly supported by the National Natural Science Foundation of China (41672240), the Innovation Scientists and Technicians Troop Construction Projects of Henan Province (CXTD2016053), the Fundamental Research Funds for the Universities of Henan Province (NSFRF1611), Doctoral Fund of Henan Polytechnic University (B2012-106), and China Scholarship Council (201807770012).

DATA AVAILABILITY STATEMENT

All relevant data are included in the paper or its Supplementary Information.

REFERENCES

Abdelhay, A., Al Bsoul, A., Al-Othman, A., Al-Ananzeh, N. M., Jum'h, I. & Al-Taani, A. A. 2018 Kinetic and thermodynamic study of phosphate removal from water by adsorption onto (Arundo donax) reeds. *Adsorpt. Sci. Technol.* **36** (1–2), 46–61. https://doi.org/10.1177%2F0263617416684347.

Adenuga, A. A., Amos, O. D., Oyekunle, J. A. O. & Umukoro, E. H. 2019 Adsorption performance and mechanism of a low-cost biosorbent from spent seedcake of Calophyllum inophyllum in simultaneous cleanup of potentially toxic metals from industrial wastewater. *J. Environ. Chem. Eng.* **7**, 103317. https://doi.org/10.1016/j.jece.2019.103317.

Al-Ananzeh, N. M. 2021 Treatment of wastewater from a dairy plant by adsorption using synthesized copper oxide nanoparticles: kinetics and isotherms modeling optimization. *Water Sci. Technol.* **83** (7), 1591–1604. https://doi.org/10.2166/wst.2021.089.

Amankwaa, G., Yin, X. F., Zhang, L. M., Huang, W. H., Cao, Y. F., Ni, X. N. & Gyimah, E. 2021 Spatial distribution and eco-environmental risk assessment of heavy metals in surface sediments from a crater lake (Bosomtwe/Bosumtwi). *Environ. Sci. Pollut. Res.* **28**, 19367–19380. https://doi.org/10.1007/s11356-020-12112-0.

Basack, S., Bhattacharya, A. K. & Maity, P. 2014 A coastal groundwater management model with Indian case study. *Water Manage.* **167**, 126–140. http://dx.doi.org/10.1680/wama.12.00008.

Chen, Z. X. & Pan, K. 2021 Enhanced removal of Cr(VI) via in-situ synergistic reduction and fixation by polypyrrole/sugarcane bagasse composites. *Chemosphere* **272**, 129606. https://doi.org/10.1016/j.chemosphere.2021.129606.

Chu, Y., Liu, S. Y., Wang, F., Bian, H. L. & Cai, G. J. 2018 Electric conductance response on engineering properties of heavy metal polluted soils. *J. Environ. Chem. Eng.* **6**, 5552–5560. https://doi.org/10.1016/j.jece.2018.08.046.

Guan, J. N., Wang, J., Pan, H., Yang, C., Qu, J., Lu, N. & Yuan, X. 2018 Heavy metals in Yinma River sediment in a major Phaeozems zone. Northeast China: Distribution, chemical fraction, contamination assessment and source apportionment. *Sci. Rep.-UK* **8**, 12231. https://doi.org/10.1038/s41598-018-30197-z.

Hassimi, H., Taleb, A., Bouezmarni, M., Karzazi, O., Taleb, M., Kherbeche, A. & Debbaut, V. 2019 The effect of the physicochemical conditions variations on the behavior of heavy metals trapped in polluted fluvial system sediments: the case of OuedSebou, Morocco. *Appl. Water Sci.* **9**, 17. https://doi.org/10.1007/s13201-019-0891-2.

He, Y., Li, B. B., Zhang, K. N., Li, Z., Chen, Y. G. & Ye, W. M. 2019 Experimental and numerical study on heavy metal contaminant migration and retention behavior of engineered barrier in tailings pond. *Environ. Pollut.* **252**, 1010–1018. https://doi.org/10.1016/j.envpol.2019.06.072.

Hu, H., Jin, Q. & Kavan, P. 2014 A study of heavy metal pollution in China: current status, pollution-control policies and countermeasures. *Sustainability* **6**, 5820–5838. https://doi.org/10.3390/su6095820.

Jafarabadi, A. R., Bakhtiari, A. R., Spanò, N. & Cappelloc, T. 2018 First report of geochemical fractionation distribution, bioavailability and risk assessment of potentially toxic inorganic elements in sediments of coral reef Islands of the Persian Gulf, Iran. *Mar. Pollut. Bull.* **137**, 185–197. https://doi.org/10.1016/j.marpolbul.2018.09.052.

Kobayashi, Y., Ogata, F., Nakamura, T. & Kawasaki, N. 2020 Synthesis of novel zeolites produced from fly ash by hydrothermal treatment in alkaline solution and its evaluation as an adsorbent for heavy metal removal. *J. Environ. Chem. Eng.* **8**, 103687. https://doi.org/10.1016/j.jece.2020.103687.

Lin, Y. P., Li, Y. H., Zheng, B. X., Yin, X. J., Wang, L., He, J. & Shu, F. F. 2019 Impact of typhoon Matmo (2014) on the distribution of heavy metals in Quanzhou Bay. *Anthropocene Coasts* **2**, 209–228. https://doi.org/10.1139/anc-2018-0006.

López, J. J., Echeverría, J., Martín, I. S. & Delgado, O. 2020 Dynamic testing in columns for soil heavy metal removal for a car park SUDS. *Sci. Total Environ.* **738**, 140229. https://doi.org/10.1016/j.scitotenv.2020.140229.

Lu, F., Zhang, H. Q., Jia, Y. G., Liu, W. Q. & Wang, H. 2019 Migration and diffusion of heavy metal Cu from the interior of sediment during wave-induced sediment liquefaction process. *J. Mar. Sci. Eng.* **7**, 449. https://doi:10.3390/jmse7120449.

Martin, J. A. R., Arana, C. D., Ramos-Miras, J. J., Gil, C. & Bolud, R. 2015 Impact of 70 years urban growth associated with heavy metal pollution. *Environ. Pollut.* **196**, 156–163. https://doi.org/10.1016/j.envpol.2014.10.014.

Pedersen, K. B., Lejon, T., Jensen, P. E. & Ottosen, L. M. 2017 The influence of sediment properties and experimental variables on the efficiency of electrodialytic removal of metals from sediment. *J. Environ. Chem. Eng.* **5**, 5312–5321. http://dx.doi.org/10.1016/j.jece.2017.10.031.

Shi, X. L. & Zhang, W. 2018 Experimental study on release of heavy metals in sediment under hydrodynamic conditions. 2018 IOP Conf. Ser.: Earth Environ. Sci. **208**, 012040. https://doi:10.1088/1755-1315/208/1/012040.

Song, J. X., Yang, X. G., Zhang, J. L., Long, Y. Q., Zhang, Y. & Zhang, T. F. 2015 Assessing the variability of heavy metal concentrations in liquid-solid two-phase and related environmental risks in the Weihe River of Shaanxi Province, China. *Int. J. Environ. Res. Public Health* **12**, 8243–8262. https://doi.org/10.3390/ijerph120708243.

Superville, P. J., Prygiel, E., Magnier, A., Lesven, L., Gao, Y., Baeyens, W., Ouddane, B., Dumoulin, D. & Billon, G. 2014 Daily variations of Zn and Pb concentrations in the Deûle River in relation to the resuspension of heavily polluted sediments. *Sci. Total Environ.* **470–471**, 600–607. http://dx.doi.org/10.1016/j.scitotenv.2013.10.015.

Tang, W. Z., Shan, B. Q., Zhang, H., Zhang, W. Q., Zhao, Y., Ding, Y. K., Rong, N. & Zhu, X. L. 2014 Heavy metal contamination in the surface sediments of representative limnetic ecosystems in Eastern China. *Sci. Rep.-UK* **4**, 7152. http://dx.doi.org/10.1038/srep07152.

Wang, X. R., Li, L., Yan, X. H., Meng, X. G. & Chen, Y. C. 2020 Processes of chromium (VI) migration and transformation in chromate production site: a case study from the middle of China. *Chemosphere* **257**, 127282. https://doi.org/10.1016/j.chemosphere.2020.127282.

Won, J., Wirth, X. & Burns, S. E. 2019 An experimental study of cotransport of heavy metals with kaolinite colloids. *J. Hazard. Mater.* **373**, 476–482. https://doi.org/10.1016/j.jhazmat.2019.03.110.

Zhang, Y. H., Zhang, H. H., Zhang, Z. B., Liu, C. Y., Sun, C. Z., Zhang, W. & Marhaba, T. 2018 pH effect on heavy metal release from a polluted sediment. *J. Chem.-NY.*, 7597640. https://doi.org/10.1155/2018/7597640.

Zhao, Y. Q. & Yang, Y. 2007 Effect of vertical movement of river pollutants on groundwater quality. *Environ. Pollut. Control* **29** (2), 110–114 (in Chinese).

First received 4 March 2021; accepted in revised form 26 July 2021. Available online 9 August 2021